He, P. and Newson, T. (2020) ***Géotechnique Letters* 10**, 1–5, https://doi.org/10.1680/jgele.19.00016

Undrained capacity of circular foundations under combined horizontal and torsional loads

P. HE* and T. NEWSON†

Torsional loads can be significant on the shallow foundations of large onshore and offshore structures. However, the effect of torsional loads in isolation and in combination with other load directions has not been well studied. In this paper, a failure envelope for combined horizontal (H) and torsional load (T) for circular surface foundations on soils under undrained conditions has been derived using the upper-bound plasticity method. In addition, this solution is compared with finite-element model results and theoretical solutions for the uniaxial capacity for H and T. The H–T failure envelope obtained from a conventional design standard method (i.e. DNVGL-ST-0126) is also compared with the upper-bound solution. The upper-bound solution is in excellent agreement with the finite-element results, and the codified H–T failure envelope appears to be conservative compared with the other methods. This approach can help validate finite-element results and aid the assessment of the ultimate capacity of shallow circular foundations under combined horizontal and torsional loading.

KEYWORDS: bearing capacity; clays; footings/foundations

NOTATION

$\mathrm{d}\dot{E}$	rate of internal energy dissipation of a small area
e	load eccentricity
H	horizontal load
H'	equivalent horizontal load defined in DNVGL-ST-0126
H_{ult}	ultimate horizontal capacity
k	vertical rate of change of the soil undrained shear strength
l_{eff}	length of the effective area of the foundation
M	moment load
R	radius of the foundation
s_{u}	undrained shear strength of the soil
T	torsional load
T_{ult}	ultimate torsional capacity
V	vertical load
V_{ult}	ultimate vertical capacity
$\dot{W}(s)$	work rate of external forces
$\dot{\alpha}$	virtual angular velocity of the foundation

INTRODUCTION

Shallow foundations have been extensively used for the foundation design of large onshore and offshore structures, such as wind turbines, transmission towers and oil-drilling platforms. The majority of offshore foundations are circular or close to circular in form. Since these structures are generally subjected to various load combinations due to self-weight, environmental loads and accidental loads (e.g. wind, wave and snag loads), assessment of the bearing capacity of shallow foundations under complex loading is key to the ultimate limit-state design of shallow foundations.

The typical design approaches (e.g. DNV GL, 2016; API, 2011) for shallow offshore foundations involve classical solutions based on plasticity and empirical methods for determining the uniaxial vertical bearing capacity (Terzaghi, 1951). The load inclination factor and the effective foundation area are introduced to modify these methods to account for the effects of load inclination and eccentricity, respectively. However, this simple, traditional approach may not always be accurate enough for some cases, because the effects of load inclination and eccentricity are separately considered (Ukritchon *et al.*, 1998).

A more recent design approach is the failure envelope method, which explicitly incorporates the load-interaction effects of the various load components (e.g. Bransby & Randolph, 1998). This method has also been recommended as an alternative to conventional theory by API (2001) and ISO 19901-4 (ISO, 2016). The current research focuses predominantly on the interaction between vertical (V), horizontal (H) and moment loads (M). However, environmental loads on structures are often not co-planar, and transverse loads can also induce significant torsional effects on the foundation (Bienen *et al.*, 2007). Therefore, under certain conditions torsional loads should also be considered in the failure envelope method, but the effect of coupled torsion has not been well studied. Bounding methods of plasticity (i.e. lower- and upper-bound methods, Chen, 2013) and finite-element analysis has been commonly used for estimating the failure envelopes of shallow foundations. The finite-element method is attractive due to its flexibility and ability to model very complex cases. For example, Nouri *et al.* (2014) and Feng *et al.* (2016) developed H–T failure envelopes for rectangular foundations using this approach. An elliptical form of equation is often used to characterise the normalised H–T failure surface

$$\left(\frac{T}{T_{\mathrm{ult}}}\right)^{m}+\left(\frac{H}{H_{\mathrm{ult}}}\right)^{n}=1 \tag{1}$$

The power coefficients of m and n for surface square foundations are recommended to be $m = 1{\cdot}76$ and $n = 1{\cdot}71$ by Feng *et al.* (2016). Finnie & Morgan (2004) proposed

Manuscript received 15 September 2019; first decision 25 November 2019; accepted 2 December 2019.

*Geotechnical Research Centre, Department of Civil & Environmental Engineering, Western University, London, Canada (Orcid:0000-0001-7677-9370).
†Geotechnical Research Centre, Department of Civil & Environmental Engineering, Western University, London, Canada.

approximate values for m and n (equal to 1·75 for both) for circular and square foundations, based on the limit equilibrium method. Saviano & Pisanò (2017) numerically studied the effects of misalignment on the horizontal–vertical (HV) capacity of circular suction anchors for undrained conditions, however, the H–T failure envelopes and expressions for a surface foundation are not explicitly provided. In general, bounding methods of plasticity are lengthy and difficult to apply for cases with complicated geometries and loading conditions, and therefore only special cases can usually be solved. However, this is still an attractive approach, since it can provide simple analytical expressions for foundation bearing capacity that can be used in their own right, or can be used to verify the results of finite-element analysis and in some cases may be extended to more complex conditions. Nouri *et al.* (2014) and Feng *et al.* (2016) also developed upper-bound solutions for both surface and embedded foundations under combined horizontal and torsional loading. However, these studies are confined to rectangular-shaped foundations. Although the H–T failure envelope for a square foundation is expected to be similar to that of a circular foundation, there will be some differences due to the varying shapes and a rigorous investigation of the failure envelope for circular foundations appears to be missing from the literature.

The objective of this paper is therefore to derive a failure envelope for combined horizontal (H) and torsional load (T) for shallow circular surface foundations on homogeneous soils under undrained conditions using the upper-bound plasticity method. The upper-bound solution is then compared with finite-element results for both homogeneous and heterogeneous strength soils. The H–T failure envelope obtained from the method specified in DNVGL-ST-0126 (DNV GL, 2016) is also compared with the upper-bound solution.

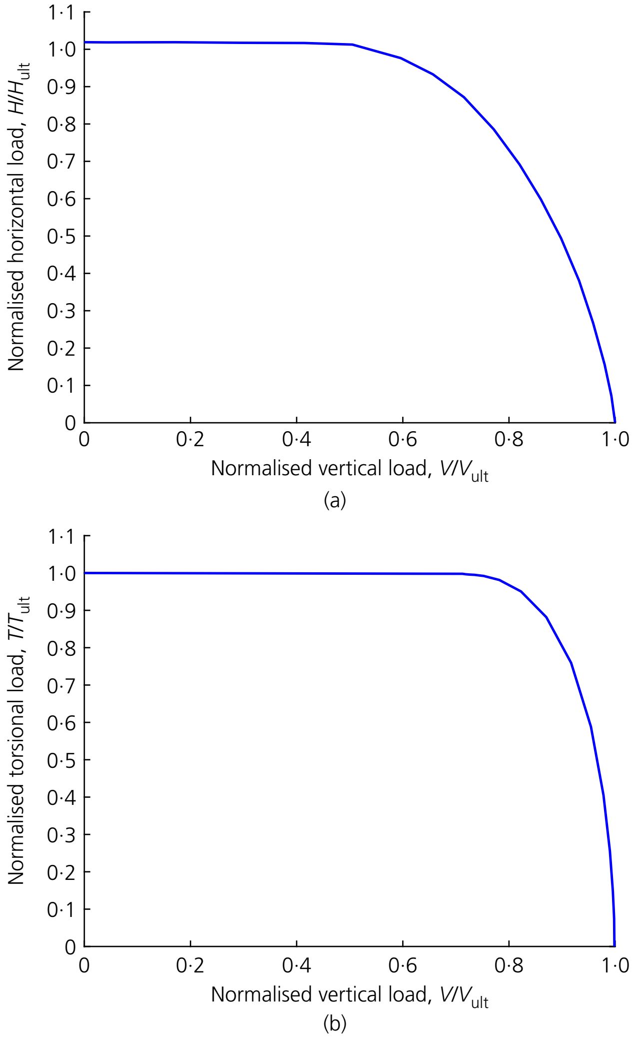

Fig. 1. H–V and T–V failure envelopes of circular surface foundations under undrained conditions: (a) H–V failure envelope (source: Shen *et al*. (2016)) and (b) T–V failure envelope (source: He & Newson (2019))

UPPER-BOUND SOLUTION

In this section, the upper-bound method of plasticity (Drucker & Prager, 1952) is utilised to determine the interaction between horizontal and torsional loads for circular surface foundations. To apply this method, a kinematically admissible collapse mechanism is assumed and the unknown forces are evaluated by equating the internal rate of energy dissipation in the plastic material to the work rate of the external forces. Minimisation of the unknown forces with respect to the predefined geometric parameters can provide an upper-bound solution for the failure envelope that will either lie above or on the true envelope.

Previous finite-element studies (e.g. Shen *et al.*, 2016; He & Newson, 2019) have demonstrated that the maximum horizontal (H) or torsional (T) forces that can be mobilised for a circular surface foundation under undrained conditions is equal to the ultimate capacity (H_{ult} or T_{ult}), when the vertical load acting on the foundation is less than half of the ultimate vertical capacity (V_{ult}) of the foundation, as shown in Fig. 1. (Although this is the case for the T–V failure envelope at $V/V_{ult} \leq 0{\cdot}70$, the range of $V/V_{ult} \leq 0{\cdot}50$ is still used in this paper considering the turning point of the H–V failure envelope equal to 0·50.) This indicates that generally the vertical load has no effect on the maximum horizontal and torsional loads that can be mobilised for a surface foundation; thus the ultimate horizontal and torsional capacities depend only on the interface resistance. Therefore, for H–T failure envelopes under a condition of $V/V_{ult} \leq 0{\cdot}50$ (often assumed in design), the failure criterion of the surface foundation under H and T loads can be reasonably assumed to involve full mobilisation of the undrained shear strength (s_u) of the soil in contact with the foundation.

Figure 2 shows the schematic of the loading and geometric configurations of a circular surface foundation. The foundation is subjected to a horizontal load, H, and a torsional load, T, simultaneously at the base centre of the foundation (point C). These two loads can be equivalently replaced with a horizontal load applied at point C, at an eccentricity of e $(= T/H)$ from C. The foundation is considered to be a rigid body and the rotation centre of the foundation is assumed to be point O, which is at a distance s from the centre of the foundation. Assuming that the virtual angular velocity of the foundation is $\dot{\alpha}$ about point O, the work rate of external forces, $\dot{W}(s)$, can be expressed as

$$\dot{W}(s) = H(s + e)\dot{\alpha} \tag{2}$$

Assuming that the upper-bound collapse mechanism involves pure translation at the soil–foundation interface and that the undrained shear strength of the soil at the interface is fully mobilised, the rate of internal energy dissipation of a small area, dA $(= r\,\mathrm{d}r\,\mathrm{d}\beta)$, can be found from (see Fig. 2)

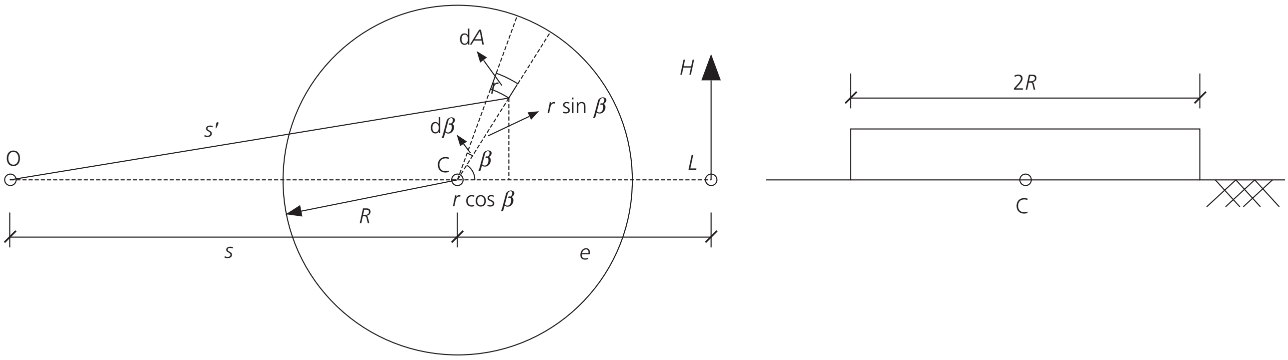

Fig. 2. Schematic of a circular foundation under horizontal and torsional loads

$$\begin{aligned} \mathrm{d}\dot{E} &= s_\mathrm{u} s' \dot{\alpha}\, \mathrm{d}A \\ &= s_\mathrm{u}\dot{\alpha}\sqrt{(s + r\cos\beta)^2 + (r\sin\beta)^2}\, r\, \mathrm{d}r\, \mathrm{d}\beta \end{aligned} \tag{3}$$

The rate of the total internal energy dissipation is equal to $\mathrm{d}\dot{E}$ integrated over the total foundation area – that is

$$\dot{E}(s) = s_\mathrm{u}\dot{\alpha}\int_0^R\int_0^{2\pi}\sqrt{(s + r\cos\beta)^2 + (r\sin\beta)^2}\, r\, \mathrm{d}r\, \mathrm{d}\beta \tag{4}$$

where R is the radius of the foundation.

Equating the internal rate of energy dissipation to the work rate of external forces can give H as a function of s

$$H(s) = \frac{\dot{E}(s)}{(s+e)\dot{\alpha}} \tag{5}$$

Minimising $H(s)$ with respect to s results in the minimum upper-bound failure load. Since only one variable is involved in equation (5), taking $\mathrm{d}H(s)/\mathrm{d}s = 0$ yields

$$\frac{\mathrm{d}\dot{E}(s)}{\mathrm{d}s} - \frac{\dot{E}(s)}{s+e} = 0 \tag{6}$$

Equation (6) implies that the optimal $s = s_0$ is a function of the horizontal eccentricity, e. It should be noted that an analytical solution of equation (6) is difficult to evaluate. Since e relates H and T by $e = T/H$, for a given e (i.e. one point on the H–T envelope), the optimal $s = s_0$ can be numerically evaluated from equation (6). Substituting the solution $s = s_0$ into equation (5), allows the optimal H for a certain e to be found

$$\begin{aligned} H &= \left.\frac{\dot{E}(s)}{(s+e)\dot{\alpha}}\right|_{s=s_0} = \left.\frac{1}{\dot{\alpha}}\frac{\mathrm{d}\dot{E}(s)}{\mathrm{d}s}\right|_{s=s_0} \\ &= s_\mathrm{u}\int_0^R\int_0^{2\pi}\frac{r(s_0 + r\cos\beta)}{\sqrt{(s_0 + r\cos\beta)^2 + (r\sin\beta)^2}}\mathrm{d}r\, \mathrm{d}\beta \end{aligned} \tag{7}$$

Based on equation (7), the horizontal load, H, can be regarded as a function of e, since s_0 is associated with e in equation (6). Moreover, equation (7) represents the failure envelope between H and T if $e = T/H$ is substituted. Although an analytical expression of equation (7) cannot be explicitly provided, the solutions for two special cases can be evaluated based on this general form: pure horizontal sliding and pure torsion of the foundation. For pure horizontal sliding, the horizontal eccentricity of the loads is zero (i.e. $e = 0$) and the lever arm of the equivalent horizontal load becomes infinity (i.e. $s_0 + e = s_0 = \infty$). Applying $s_0 = \infty$ reduces the solution to the ultimate horizontal capacity, H_ult

$$H_\mathrm{ult} = H|_{s_0=\infty} = s_\mathrm{u}\int_0^R\int_0^{2\pi}\frac{r(1 + (r/s_0)\cos\beta)}{\sqrt{(1 + (r/s_0)\cos\beta)^2 + ((r/s_0)\sin\beta)^2}}\mathrm{d}r\, \mathrm{d}\beta = s_\mathrm{u}\int_0^R\int_0^{2\pi} r\, \mathrm{d}r\, \mathrm{d}\beta = \pi R^2 s_\mathrm{u} \tag{8}$$

This expression is similar to the finite-element results obtained by Shen *et al.* (2016) and equal to the theoretical solution.

Similarly, $s = s_0 = 0$ (i.e. the foundation rotates about point C) leads to the ultimate rotational capacity, T_ult

$$T_\mathrm{ult} = He = s_\mathrm{u}\int_0^R\int_0^{2\pi} r^2\, \mathrm{d}r\, \mathrm{d}\beta = \frac{2\pi}{3}R^3 s_\mathrm{u} \tag{9}$$

which provides the same result as given by Finnie & Morgan (2004) for the theoretical solution.

More generally, the relationship between H and e can be obtained by taking a series of values of e, as shown in Fig. 3. It can be seen that the reduction of H is relatively small when e/D is less than 0·1, followed by a rapid decrease in the range of 0·1–3. At large e/D ratios (i.e. >3), the horizontal resistance of the foundation is almost negligible. The upper-bound solution of Nouri *et al.* (2014) for a square foundation is also shown in Fig. 3 for comparison. It shows that a square foundation has a slightly larger horizontal capacity than a circular foundation for a given value of load eccentricity. Applying $e = T/H$ can transform Fig. 3 to the combined failure envelope between H and T, as illustrated in Fig. 4. The curves obtained from finite-element analyses (He & Newson, 2019) for the same foundation geometry and homogeneous soil properties at $V/V_\mathrm{ult} = 0.05$ (representing the extreme case of $V/V_\mathrm{ult} = 0$, since the finite-element analysis with $V = 0$ experiences convergence issues) are also incorporated for comparison. These analyses (He & Newson, 2019), utilised a three-dimensional soil-foundation model with a zero-tension interface under combined VHMT loads. The undrained shear strength of the soil was also considered to linearly increase with depth and three vertical strength rates of change with depth were employed

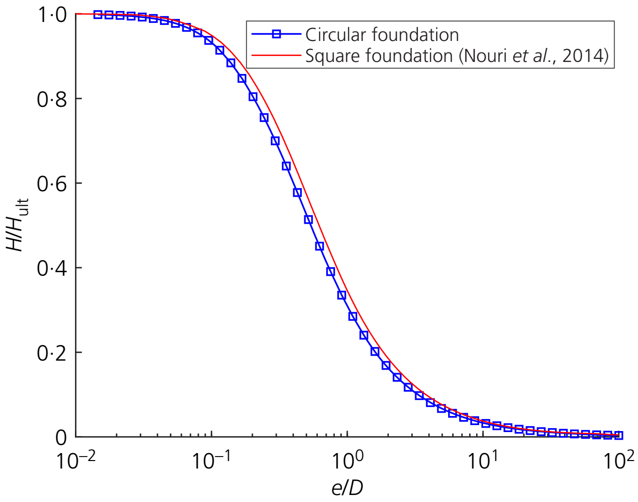

Fig. 3. Reduction of horizontal capacity with eccentricity from the upper-bound solution

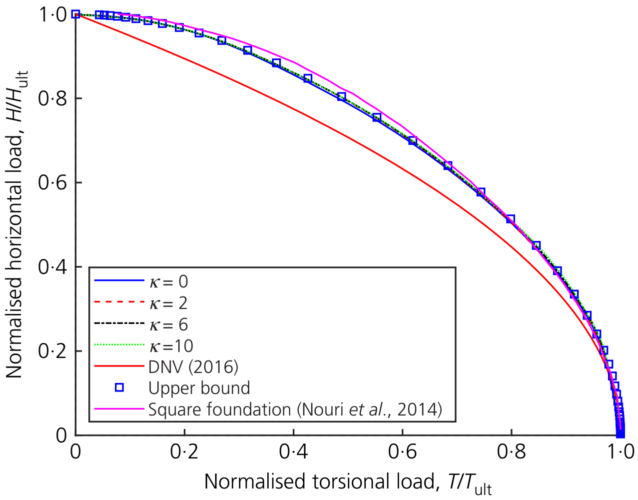

Fig. 4. Normalised *H–T* failure envelopes

(i.e. $s_u = s_{u0} + kz$, with $\kappa = kD/s_{u0}$ taken as 2, 6 and 10). In comparison, DNVGL-ST-0126 (DNV GL, 2016) recommends an equivalent horizontal force to account for the reduction in horizontal load capacity caused by torsional loads

$$H' = \frac{2T}{l_{eff}} + \sqrt{H^2 + \left(\frac{2T}{l_{eff}}\right)^2} \tag{10}$$

where l_{eff} is the length of the effective area of the foundation. For a circular foundation with the absence of moment loading, l_{eff} is equal to $\sqrt{A}$ (A is the area of the foundation). H_{ult} and T_{ult} can be calculated by equating the equivalent horizontal force to As_u and taking $T = 0$ and $H = 0$, respectively, which yields $H_{ult} = As_u$ and $T_{ult} = 1/4(As_u l_{eff})$. Equation (10) can then be rearranged to give the normalised *H–T* failure envelope

$$\left(\frac{1}{2}\frac{T}{T_{ult}}\right) + \sqrt{\left(\frac{H}{H_{ult}}\right)^2 + \left(\frac{1}{2}\frac{T}{T_{ult}}\right)^2} = 1 \tag{11}$$

and this failure envelope is plotted in Fig. 4.

Equation (1) with $m = 1{\cdot}62$ and $n = 1{\cdot}79$ can be used to approximate the proposed upper-bound solution with a coefficient of determination (R^2) of 0·99. These values are respectively lower and higher than the best estimates available in the literature of $m = n = 1{\cdot}75$ (Finnie & Morgan, 2004). It can be seen that the three-dimensional finite-element results agree well with the upper-bound solution, confirming the suitability of the collapse mechanism adopted. The finite-element results also show that the soil strength heterogeneity has no effect on the *H–T* failure envelopes, because the *H–T* bearing capacity depends only on the interface resistance. Since the exact solution is expected to be bracketed by lower and upper bounds (Chen, 2013), a lower-bound solution is required to further validate the results, but is expected to provide the same results. Moreover, DNVGL-ST-0126 (DNV GL, 2016) provides a more conservative design estimate in terms of H and T loads. It can also be seen that the reduction of H/H_{ult} for the DNV solution is almost linear with T/T_{ult} in the range of 0–0·8 and then gradually approaches the upper-bound solution. In addition, the *H–T* failure envelope for a circular foundation appears to be more conservative (difference up to 4%) than that for a square foundation (derived by Nouri *et al.*, 2014) where $T/T_{ult} < 0{\cdot}8$.

CONCLUSIONS

An *H–T* failure envelope for a circular surface foundation on a soil under undrained conditions has been derived using the upper-bound method of plasticity. This upper-bound solution is compared with the corresponding finite-element results and the *H–T* failure envelope obtained from a code-based design method in DNVGL-ST-0126 (DNV GL, 2016). The *H–T* failure envelope is not affected by the soil strength heterogeneity, and the upper-bound solution favourably compares with the finite-element results. Comparisons with failure envelopes for square foundations under the same conditions (found in the literature) show the circular foundation envelope to be more conservative. In addition, the recommended *H–T* failure envelope by DNVGL-ST-0126 (DNV GL, 2016) also appears to be conservative compared with the upper-bound and finite-element results. The proposed method provides confidence in the finite-element model results and will aid the assessment of the ultimate capacity of shallow circular foundations under combined horizontal and torsional loads.

ACKNOWLEDGEMENTS

The authors acknowledge the financial support of the Natural Sciences and Engineering Research Council (grant RGPIN-2015-06062). The first author is grateful for the financial support of the China Scholarship Council (CSC). The authors also thank the anonymous reviewers for their helpful comments and suggestions.

REFERENCES

API (American Petroleum Institute) (2011). *Geotechnical and foundation design considerations*. Washington, DC, USA: American Petroleum Institute.

Bienen, B., Gaudin, C. & Cassidy, M. J. (2007). Centrifuge tests of shallow footing behaviour on sand under combined vertical-torsional loading. *Int. J. Phys. Model. Geotech.* **7**, No. 2, 01–21.

Bransby, M. F. & Randolph, M. F. (1998). Combined loading of skirted foundations. *Géotechnique* **48**, No. 5, 637–655, https://doi.org/10.1680/geot.1998.48.5.637.

Chen, W. F. (2013). *Limit analysis and soil plasticity*. New York, NY, USA: Elsevier.

DNV GL (Det Norske Veritas GL) (2016). *DNVGL-ST-0126: Support structures for wind turbines*. Høvik, Norway: DNV GL Group.

Drucker, D. C. & Prager, W. (1952). Soil mechanics and plastic analysis or limit design. *Q. Appl. Math.* **10**, No. 2, 157–165.

Feng, X., Randolph, M. F. & Gourvenec, S. (2016). An analytical solution for the undrained horizontal–torsional resistance of mudmats. *Géotechnique* **67**, No. 4, 325–337, https://doi.org/10.1680/jgeot.16.P.026.

Finnie, I. M. S. & Morgan, N. (2004). Torsional loading of subsea structures. In *The 4th international offshore and polar engineering conference* (eds J. S. Chung, K. Izumiyama, M. Sayed and S. W. Hong), pp. 326–333. Toulon, France: International Society of Offshore and Polar Engineers.

He, P. P. & Newson, T. (2019). Undrained capacity of circular shallow foundations under combined VHMT loading. In *The 16th Pan-American conference on soil mechanics and geotechnical engineering* (eds N. P. López-Acosta, E. Martínez-Hernández, A. L. Espinosa-Santiago, J. A. Mendoza-Promotor and A. O. López), pp. 1018–1025. Cancun, Mexico: International Society for Soil Mechanics and Geotechnical Engineering.

ISO (International Standards Organisation) (2016). *ISO 19901-4: Petroleum and natural gas industries – specific requirements for offshore structures – part 4: Geotechnical and foundation design considerations*, 2nd edn. Geneva, Switzerland: ISO.

Nouri, H., Biscontin, G. & Aubeny, C. P. (2014). Undrained sliding resistance of shallow foundations subject to torsion. *J. Geotech. Geoenviron. Engng* **140**, No. 8, 04014042.

Saviano, A. & Pisanò, F. (2017). Effects of misalignment on the undrained HV capacity of suction anchors in clay. *Ocean Engng* **133**, 89–106.

Shen, Z. C., Feng, X. W. & Gourvenec, S. (2016). Undrained capacity of surface foundations with zero-tension interface under planar VHM loading. *Comput. Geotech.* **73**, 47–57.

Terzaghi, K. (1951). *Theoretical soil mechanics.* New York, NY, USA: Wiley.

Ukritchon, B., Whittle, A. J. & Sloan, S. W. (1998). Undrained limit analyses for combined loading of strip footings on clay. *J. Geotech. Geoenviron. Engng* **124**, No. 3, 265–276.

HOW CAN YOU CONTRIBUTE?

To discuss this paper, please submit up to 500 words to the editor at journals@ice.org.uk. Your contribution will be forwarded to the author(s) for a reply and, if considered appropriate by the editorial board, it will be published as a discussion in a future issue of the journal.